Electronic Supplementary Material (ESI) for Journal of Materials Chemistry B.

Biodegradable electroactive polymers for electrochemically-triggered drug delivery

John G. Hardy, [a,b*] David J. Mouser, [a] Netzahualcóyotl Arroyo-Currás,[c] Jacqueline K. Chow, [a] Lindsey Nguy, [a] Jong M. Kim [a] and Christine E. Schmidt [a,b*]

[a] Department of Biomedical Engineering, The University of Texas at Austin, Austin, TX 78712, United States of America.

[b] J. Crayton Pruitt Family Department of Biomedical Engineering, University of Florida, Biomedical Sciences Building JG-53, P.O. Box 116131, Gainesville, FL 32611-6131, United States of America.

[c] Center for Electrochemistry, Chemistry Department, The University of Texas at Austin, Austin, TX78712, United States of America.

Email: johnhardyuk@gmail.com or schmidt@bme.ufl.edu

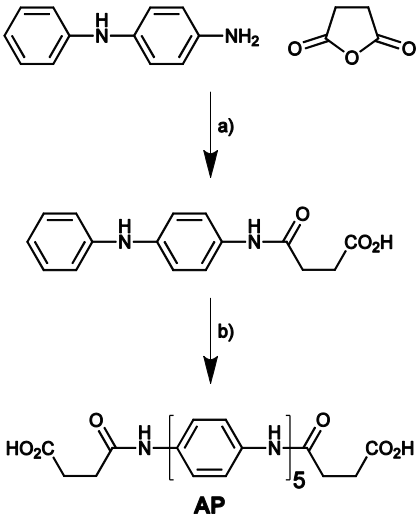

Scheme S1 Synthesis of the aniline pentamers incorporated in the electroactive polyesters. a) DCM, 24 h, r.t.; b) *p*-phenylenediamine, DMF, H_2O, HCl, $(NH_4)_2S_2O_8$, 1h, 0 °C.

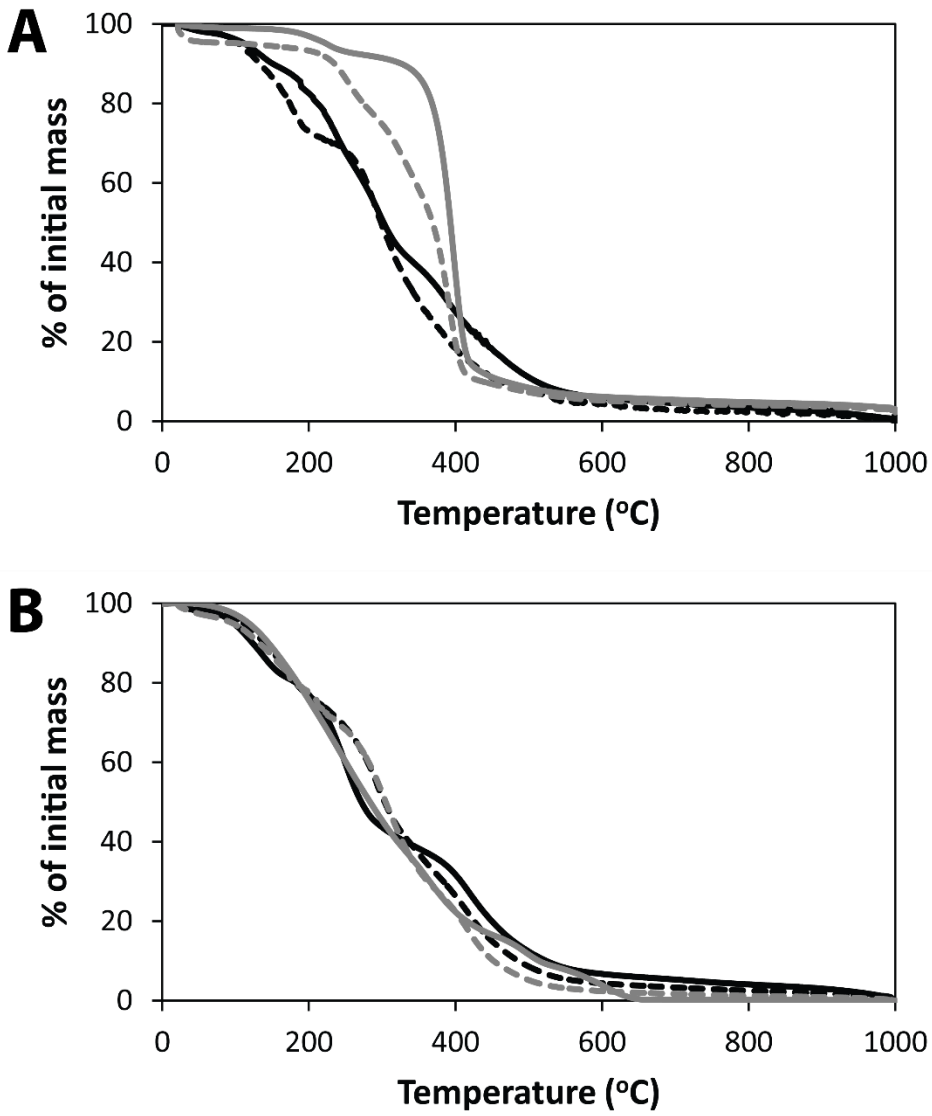

Fig. S1 TGA mass loss profiles of the electroactive polyesters. A) Polyester 1 undoped, black line; polyester 1 doped with CSA, dashed black line; polyester 2 undoped, grey line; polyester 2 doped with CSA, dashed grey line; B) polyester 3 undoped, black line; polyester 3 doped with CSA, dashed black line; polyester 4 undoped, grey line; polyester 4 doped with CSA, dashed grey line.

Table S1 Polyester compositions as determined by TGA.

	Polyester **1**	Polyester **2**	Polyester **3**	Polyester **4**
AP content (wt %)	61.5 (62.6)[a]	22.0 (25.1)[a]	56.7 (55.8)[a]	27.5 (25.1)[a]
PEG content (wt %)	38.5 (37.4)[a]	78.0 (74.9)[a]	N/A[b]	N/A[b]
PCL content (wt %)	N/A[b]	N/A[b]	43.3 (44.2)[a]	72.5 (74.9)[a]

[a]) Theoretical content based upon a 1:1 ratio of carboxylic acid-terminated aniline pentamers (APs) and alcohol-terminated poly(ethylene glycol)s (PEGs) or poly(caprolactone)s (PCLs). b) Not applicable.

Table S2 Polyester solubilities in various solvents

	Polyester **1**	Polyester **2**	Polyester **3**	Polyester **4**
Acetone	SS	SS	SS	I
Chloroform	SS	SS	SS	SS
Dichloromethane	SS	SS	SS	SS
Dimethylformamide	I	I	I	I
Dimethyl sulfoxide	S[a,c]	S[a,c]	S[a,c]	S[a,c]
Ethanol	SS	SS	SS	SS
Hexanes	I	I	I	I
Hexafluoroisopropanol	S[b,c]	S[b,c]	S[b,c]	S[b,c]
Methanol	SS	SS	SS	SS
N-methyl-2-pyrrolidone	S[a,c]	S[a,c]	S[a,c]	S[a,c]
Tetrahydrofuran	SS	SS	SS	SS
Water	I	I	I	I
Hater/HCl (1M)	SS	SS	SS	SS

I) Insoluble; sparingly soluble (SS, $0 \leq 1$ mg/mL); soluble (S, > 1 mg/mL). [a]) Samples filtered quickly through a Durapore® poly(vinylidenedifluoride) (PVDF) membrane filter unit with a pore size of 220 nm (filtration was swift to prevent dissolution of the membrane). [b]) Samples were centrifuged in polypropylene microcentrifuge tubes (Fisher Scientific, USA) at 6000 rpm for 15 minutes in a microcentrifuge (Eppendorf, USA) prior to DLS. [c]) Dynamic light scattering (DLS) experiments carried out in quartz cuvettes (Hellma, USA) using a Zetasizer Nano ZS (Malvern Instruments Ltd, UK) indicated the presence of particles with heterogeneous size distributions (data not shown).

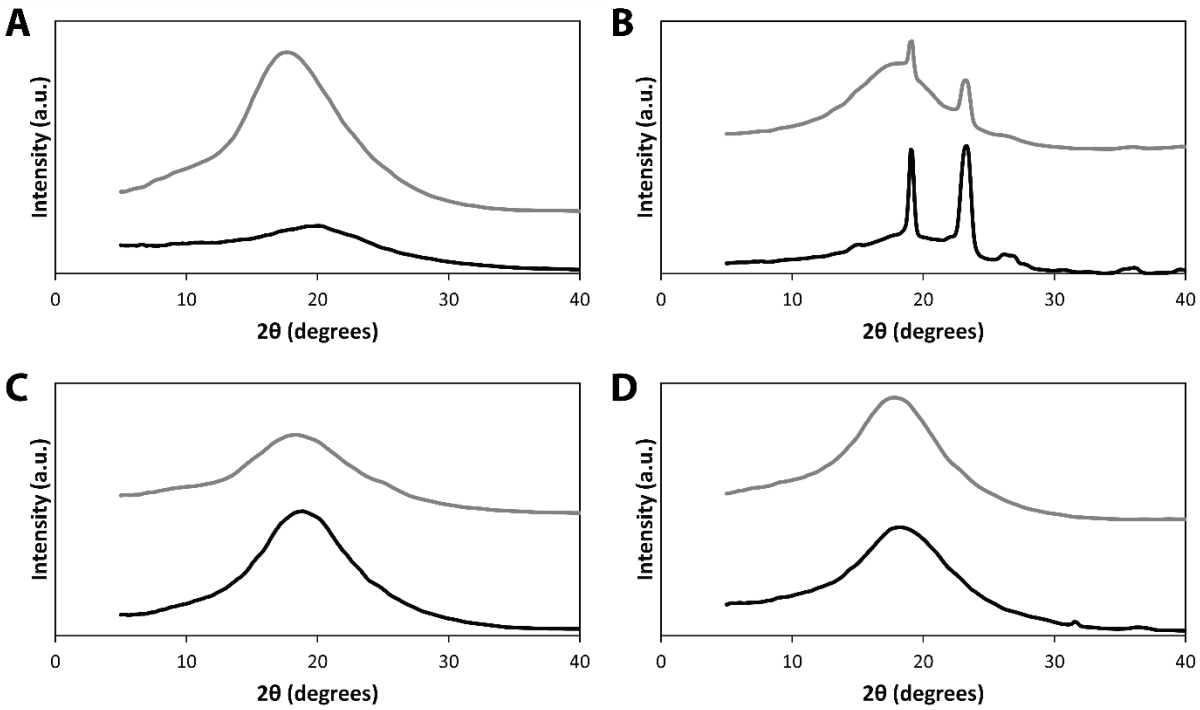

Fig. S2 XRD spectra of the electroactive polyesters. A) Polyester 1 undoped, black line; polyester 1 doped with CSA, grey line; B) polyester 2 undoped, black line; polyester 2 doped with CSA, grey line; C) polyester 3 undoped, black line; polyester 3 doped with CSA, grey line; D) polyester 4 undoped, black line; polyester 4 doped with CSA, grey line.

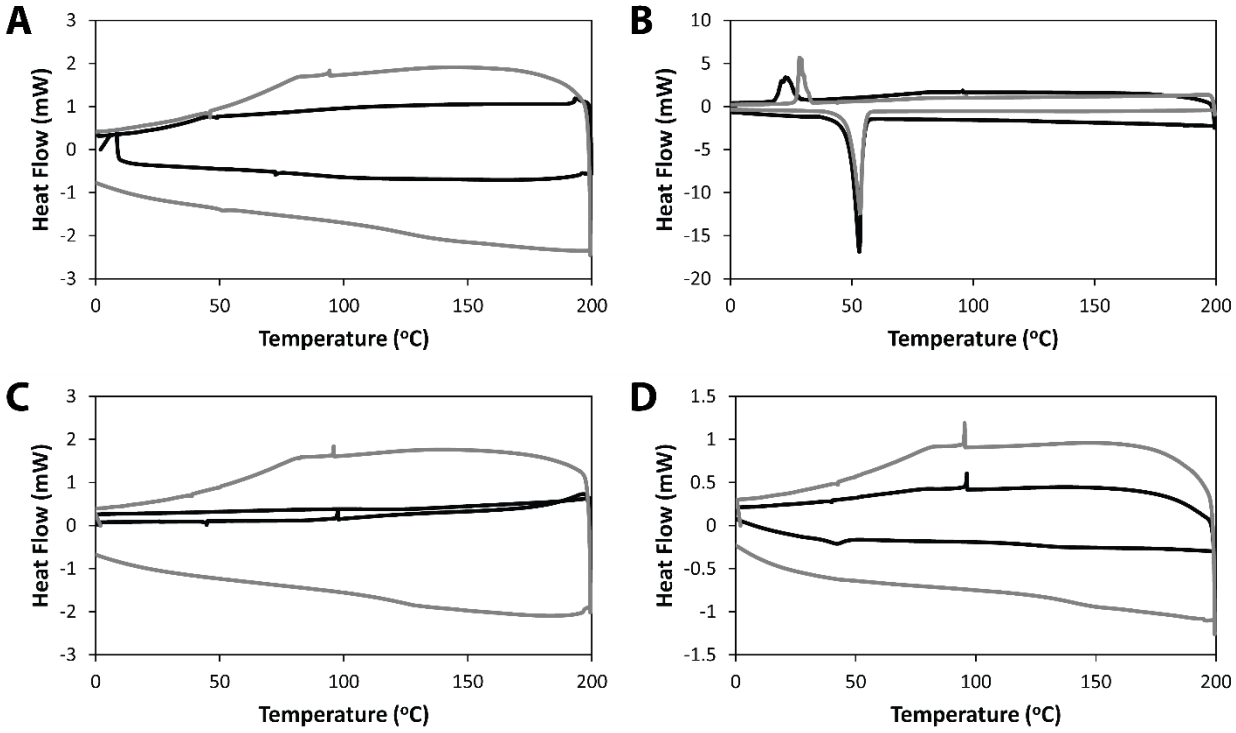

Fig. S3 DSC thermographs of the second heating/cooling cycle of the electroactive polyesters. A) Polyester **1** undoped, black line; polyester 1 doped with CSA, grey line; B) polyester **2** undoped, black line; polyester 2 doped with CSA, grey line; C) polyester **3** undoped, black line; polyester 3 doped with CSA, grey line; D) polyester **4** undoped, black line; polyester 4 doped with CSA, grey line.

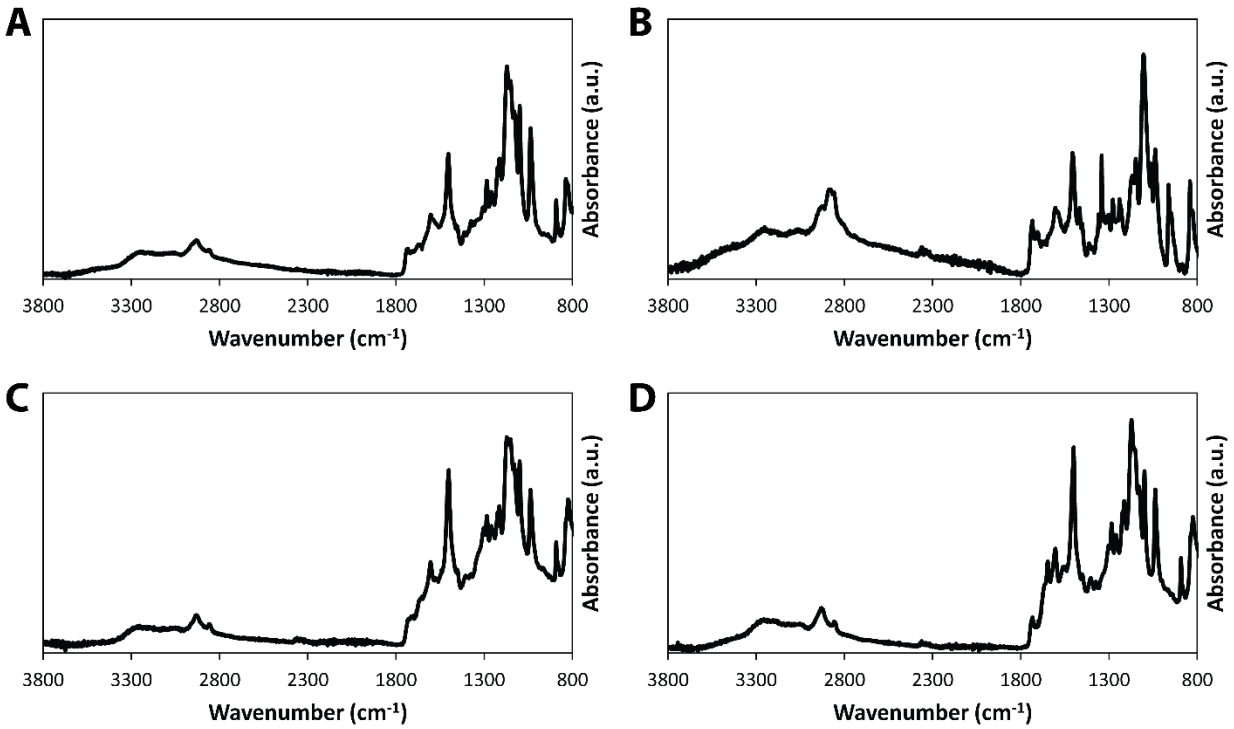

Fig. S4 FT-IR spectra of the electroactive polyesters doped with CSA. A) Polyester **1** doped with CSA; B) polyester **2** doped with CSA; C) polyester **3** doped with CSA; D) polyester **4** doped with CSA. Peaks at ca. 3293 cm^{-1} correspond to the amide NH bonds in the AP blocks; peaks at ca. 2920 and 2849 cm^{-1} correspond to the alkyl CH bonds in the backbones of the polymers; peaks at 1732 cm^{-1} correspond to ester bonds; peaks at ca. 1650 cm^{-1} correspond to the amide C=O bonds in the AP blocks, peaks at ca. 1597 and 1504 cm^{-1} correspond to the quinoid and benzenoid rings in the AP blocks.

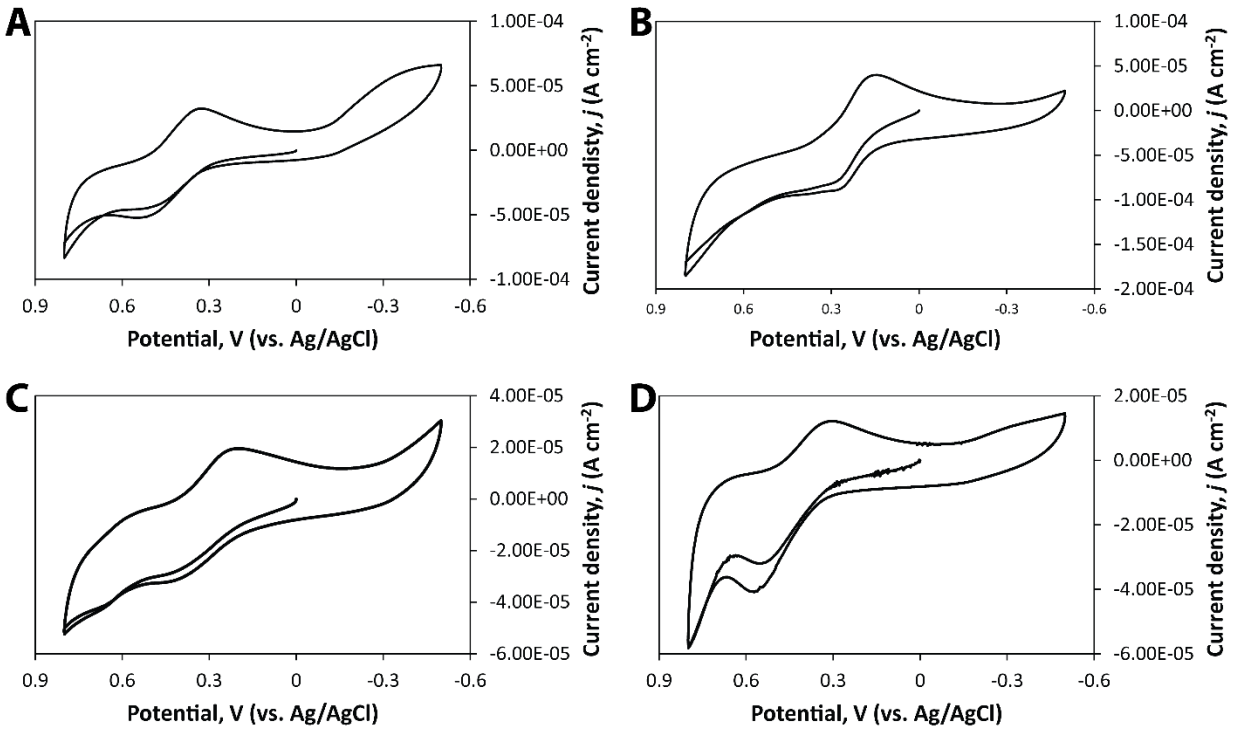

Fig. S5 Voltammograms of metastable solutions of HCl-doped polyesters in DMSO/PBS. A) Polyester **1** doped with HCl; B) polyester **2** doped with HCl; C) polyester **3** doped with HCl; D) polyester **4** doped with HCl. Scan rate = 20 mV s^{-1}.

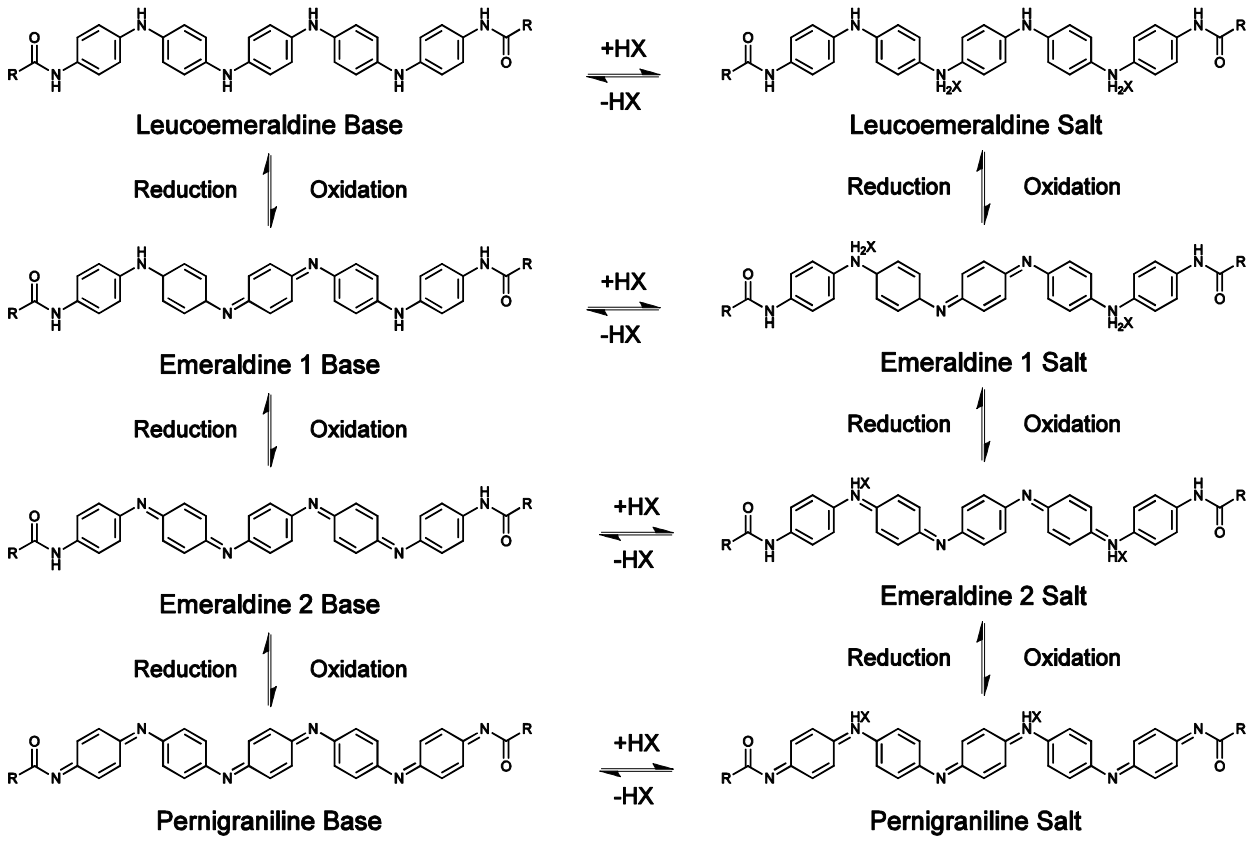

Scheme S2 Oligoaniline pH and oxidation/reduction dependent interconversion. Only the emeraldine salt is conducting. X represents an arbitrary conjugate base; in this manuscript, the conjugate bases of hydrochloric acid (HCl), camphorsulfonic acid (CSA) or dexamethasone phosphate (DMP).

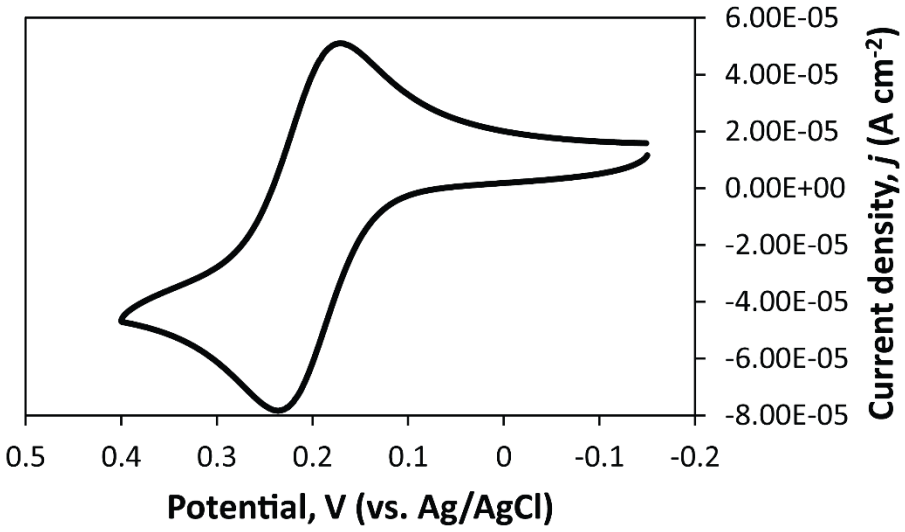

Fig. S6 Voltammogram of 0.6 mM ferrocenemethanol in 0.1 M KCl. Scan rate = 10 mV s^{-1}. See the literature for a comparison: A. Heras, A. Colina, J. Lopez-Palacios, A. Kaskela, A. Nasibulin, V. Ruiz, E. Kauppinen, *Electrochem. Commun.* 2009, 11, 442-445.

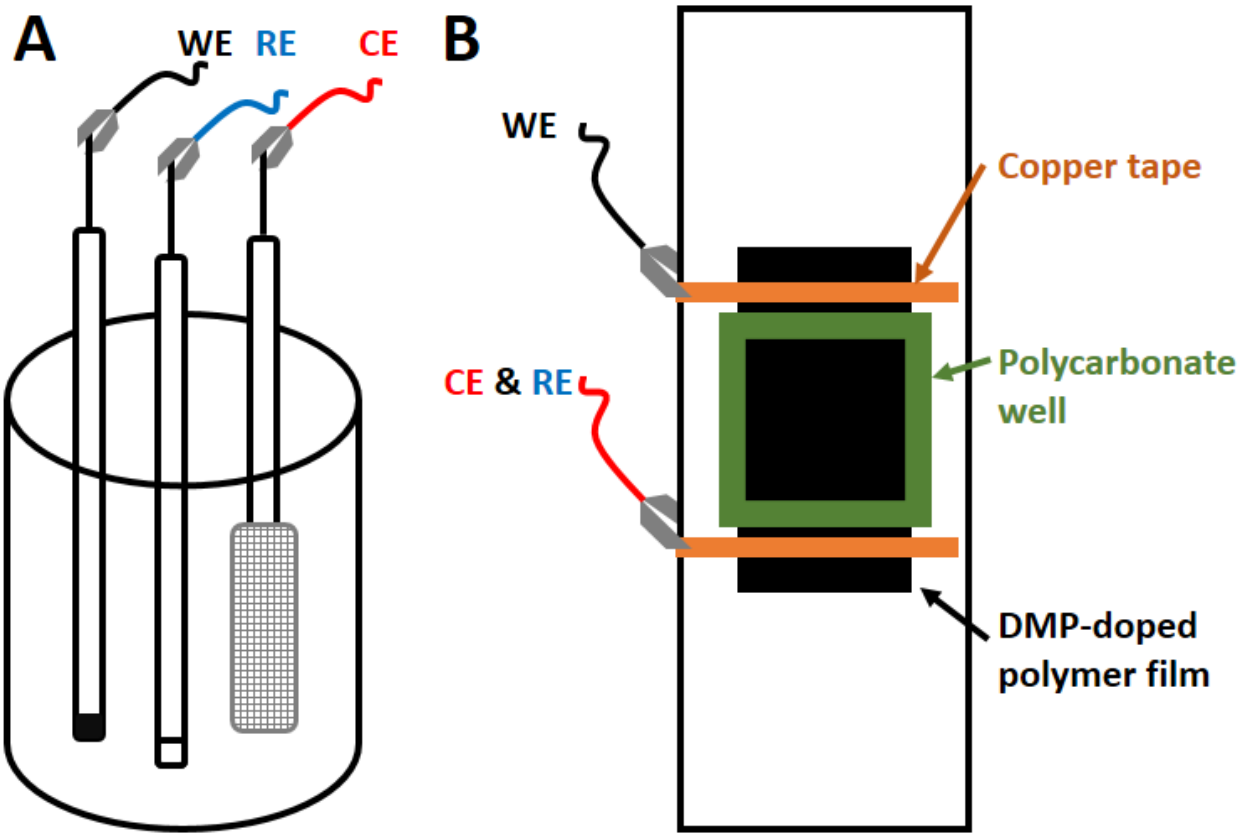

Fig. S7 A) Experimental setup for electrochemically-triggered drug delivery via potential cycling. Pt mesh counter electrode (CE), Ag/AgCl reference electrode (RE), DMP-doped polymer film coated on a glassy carbon working electrode (WE). B) Experimental setup for electrochemically-triggered drug delivery via a potential step. Counter electrode (CE), reference electrode (RE), working electrode (WE).

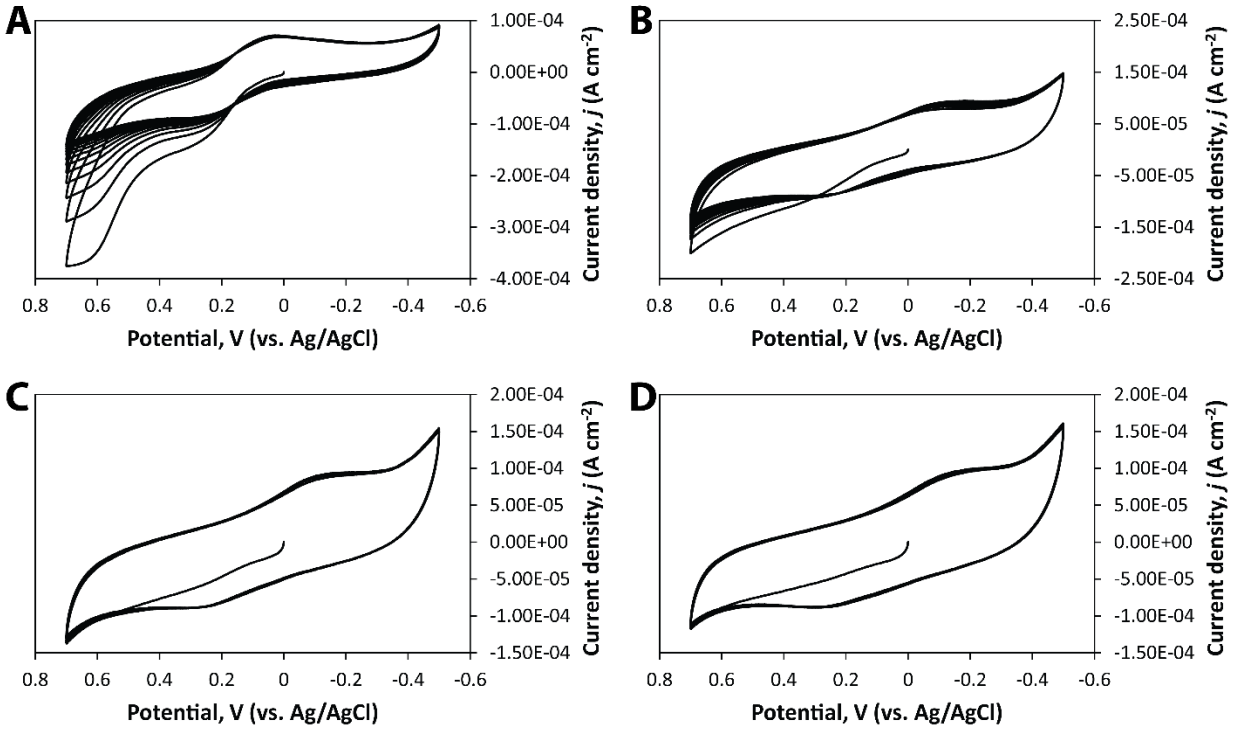

Fig. S8 Voltammograms of DMP-doped films of polyester **1** on glassy carbon electrodes in PBS demonstrating electrochemically-triggered release of the DMP, evident from the sequentially diminished current densities during repetitive potential cycling of the films, particularly noticeable in A and B. A) cycles 1 to 12. B) cycles 13 to 24. C) cycles 25 to 36. D) cycles 37 to 48. Scan rate = 50 mV s^{-1}.

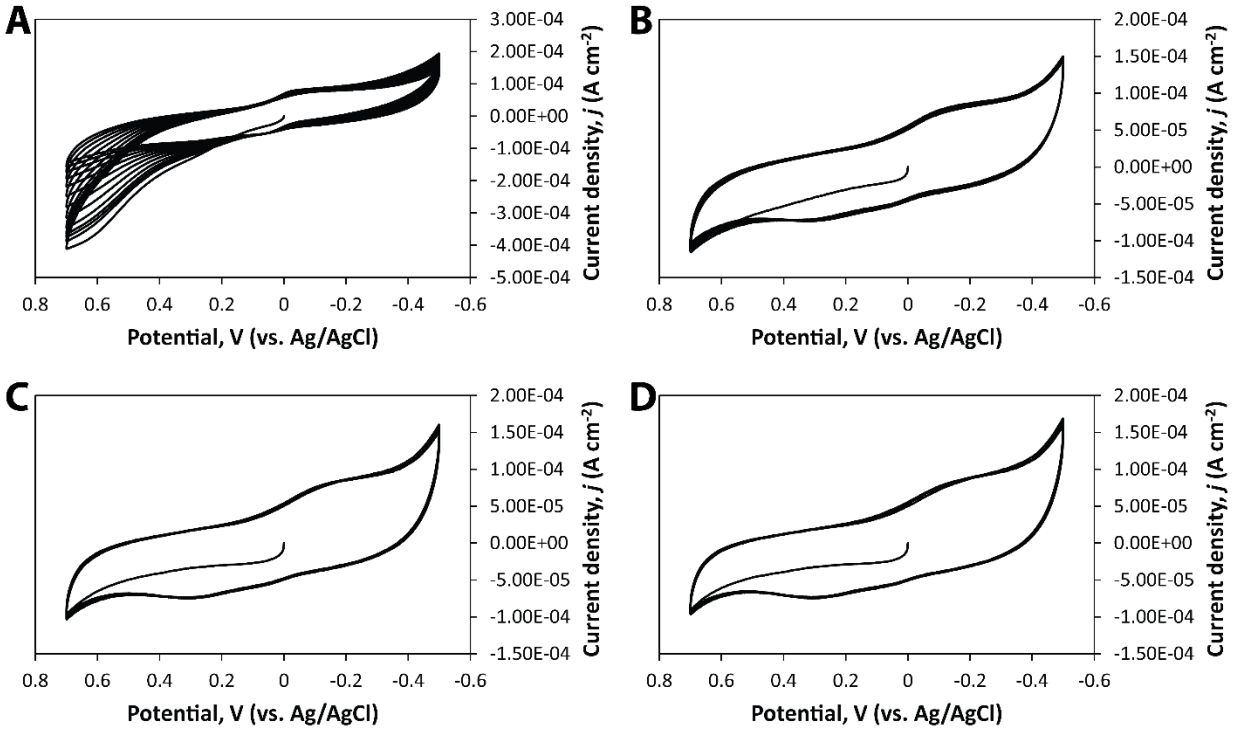

Fig. S9 Voltammograms of DMP-doped films of polyester **2** on glassy carbon electrodes in PBS demonstrating electrochemically-triggered release of the DMP, evident from the sequentially diminished current densities during repetitive potential cycling of the films, particularly noticeable in A and B. A) cycles 1 to 12. B) cycles 13 to 24. C) cycles 25 to 36. D) cycles 37 to 48. Scan rate = 50 mV s^{-1}.

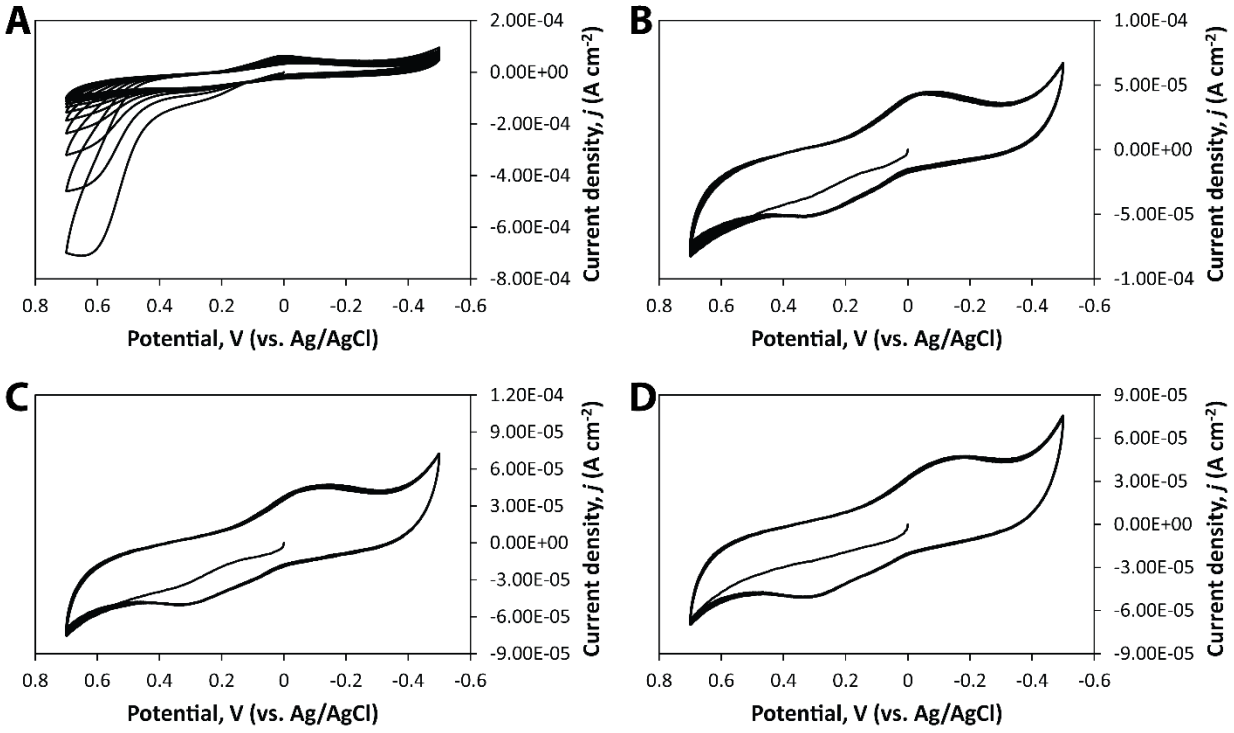

Fig. S10 Voltammograms of DMP-doped films of polyester **3** on glassy carbon electrodes in PBS demonstrating electrochemically-triggered release of the DMP, evident from the sequentially diminished current densities during repetitive potential cycling of the films, particularly noticeable in A and B. A) cycles 1 to 12. B) cycles 13 to 24. C) cycles 25 to 36. D) cycles 37 to 48. Scan rate = 50 mV s^{-1}.

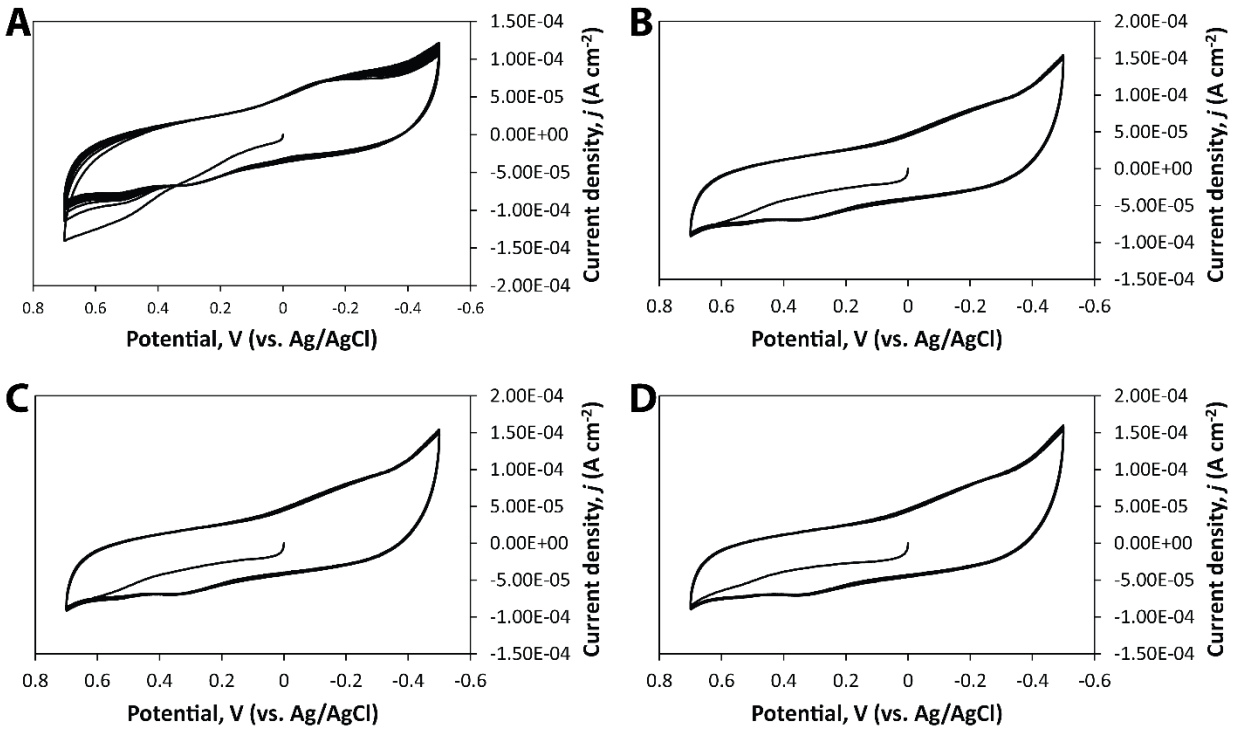

Fig. S11 Voltammograms of DMP-doped films of polyester **4** on glassy carbon electrodes in PBS demonstrating electrochemically-triggered release of the DMP, evident from the sequentially diminished current densities during repetitive potential cycling of the films, particularly noticeable in A and B. A) cycles 1 to 12. B) cycles 13 to 24. C) cycles 25 to 36. D) cycles 37 to 48. Scan rate = 50 mV s^{-1}.

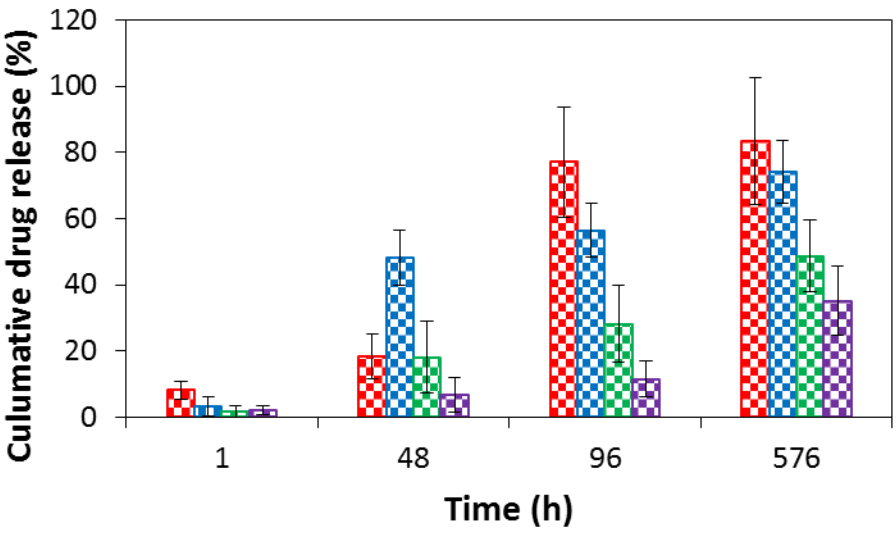

Fig. S12 Release of DMP from films of polyesters 1-4 in PBS without electrochemical stimulation. From left to right: polyester 1 (red checked bars); polyester 2 (blue checked bars); polyester 3 (green checked bars); polyester 4 (purple checked bars).

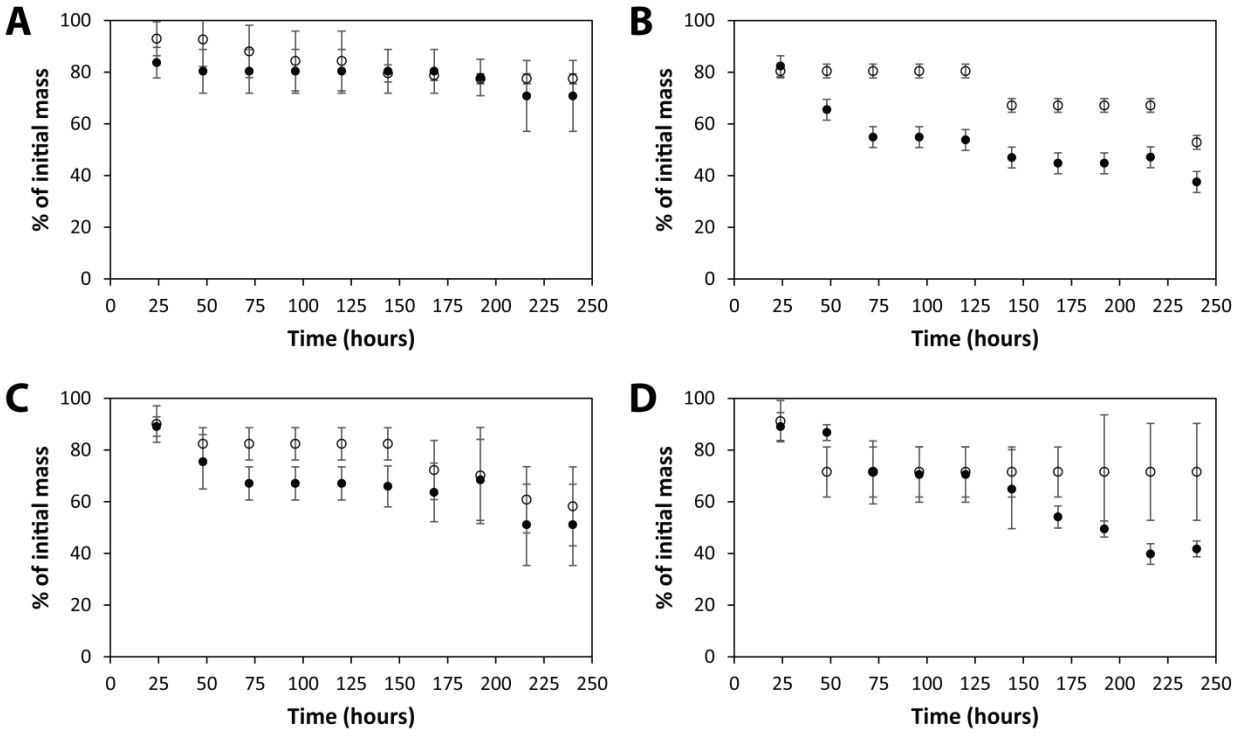

Fig. S13 In vitro degradation of the films of undoped polyesters **1**-**4** in PBS in the absence (hollow circles) or presence (filled circles) of cholesterol esterase (4 units/mL). A) Polyester **1**; B) polyester **2**; C) polyester **3**; D) polyester **4**.

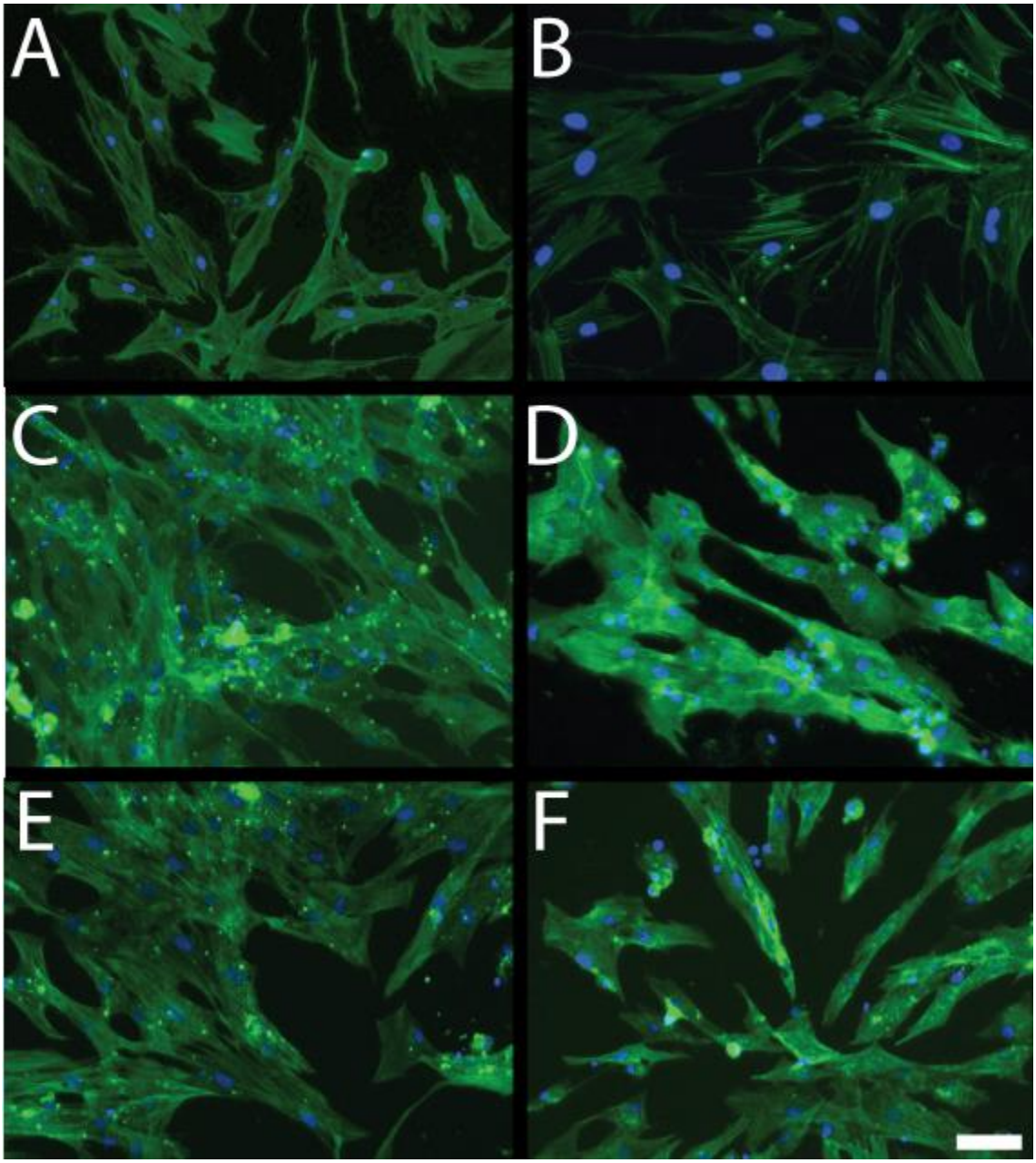

Fig. S14 Cell adhesion on various electroactive surfaces after 48 hours in culture. A) human dermal fibroblasts (HDFs) on indium tin oxide (ITO); B) human Mesenchymal stem cells (HMSCs) on ITO; C) HDFs on polyester **2** doped with CSA at a mole ratio of 1:1 CSA:AP; D) HMSCs on polyester **2** doped with CSA at a mole ratio of 1:1 CSA:AP; E) HDFs on polyester **4** doped with CSA at a mole ratio of 1:1 CSA:AP; F) HMSCs on polyester **4** doped with CSA at a mole ratio of 1:1 CSA:AP. Actin filaments within cells were stained green with Alexa Fluor 488 ® Phalloidin and nuclei within cells were stained blue with DAPI. The scale bar represents 100 µm.

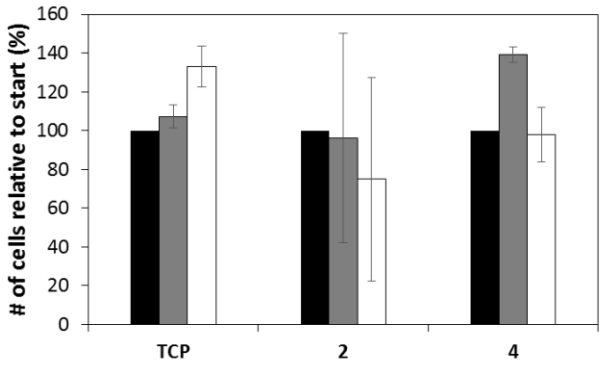

Fig. S15 Assessment of the cell viability of human dermal fibroblasts on various surfaces after 2 and 4 days in culture as determined using an AlamarBlue® Assay Kit. Black bar) Day 0. Grey bar) Day 2. White bar) Day 4.